Effect of Bone Morphogenetic Protein-7 on Steroid-induced Extracellular Matrix Synthesis in Human Trabecular Meshwork Cells.

Kim, Eun Woo

Department of Medicine
Graduate School
Yonsei University

Effect of Bone Morphogenetic Protein-7 on Steroid-induced Extracellular Matrix Synthesis in Human Trabecular Meshwork Cells.

Advisor Kim, Chan Yun

A Dissertation Submitted
to the Department of Medicine
and the Graduate School of Yonsei University
in partial fulfillment of the
requirements for the degree of
Doctor of Philosophy in Medical Science

Kim, Eun Woo

July 2025

Effect of Bone Morphogenetic Protein-7 on Steroid-induced Extracellular Matrix Synthesis in Human Trabecular Meshwork Cells.

This certifies that the Dissertation of Kim, Eun Woo is approved

Thesis Supervisor	Kim, Chan Yun
Thesis Committee Member	Byeon, Suk Ho
Thesis Committee Member	Koh, Hong
Thesis Committee Member	Kim, Joon Mo
Thesis Committee Member	Bae, Hyoung Won

Department of Medicine
Graduate School
Yonsei University
December 2024

ACKNOWLEDGEMENTS

I wish to extend my heartfelt gratitude to my thesis supervisor, Professor Chan Yun Kim. His unwavering encouragement and support were the driving force that motivated me through the challenging moments of this dissertation. Without his insightful guidance and uplifting words, I would not have had the strength or determination to see through the completion of this endeavor.

I also wish to thank Jin Ok Choi for their invaluable assistance in conducting the statistical analyses.

Finally, I wish to thank Professors Suk Ho Byeon, Hong Koh, Joon Mo Kim, and Hyoung Won Bae for their invaluable guidance, constructive criticism, and constant encouragement. Their mentorship played a pivotal role in realizing this dissertation, and I am truly indebted to them for their contributions to my academic journey.

TABLE OF CONTENTS

LIST OF FIGURES iii

LIST OF TABLES iv

ABSTRACT IN ENGLISH v

1. INTRODUCTION 1

2. MATERIALS AND METHODS 3

2.1. Animals 3

2.2. mPTD-BMP-7 preparation 3

2.3. Steroid and mPTD-BMP-7 treatment of rabbits 3

2.4. Histological examination 4

2.5. Isolation and culture of HTMCs 4

2.6. Treating HTMCs with steroid and mPTD-BMP-7 4

2.7. Imaging the ECM 5

2.8. Protein extraction and western blot analysis 5

2.9. RNA extraction and RT-qPCR 6

2.10. RNA-sequencing and analysis 8

2.11. Statistical analysis 9

3. RESULTS 10

3.1. Effects of steroid and mPTD-BMP-7 on TGF-β levels in rabbit aqueous humor and TM tissue 10

3.2. Impact of steroid and mPTD-BMP-7 treatment on the ECM of HTMCs 11

3.3. Alterations in ECM volume upon steroid and mPTD-BMP-7 co-treatment in HTMCs · 14

3.4. Effect of steroid and mPTD-BMP-7 co-treatment on rabbit TM ····· 17

3.5. Identification of differential mRNA expression in HTMCs treated with steroid and mPTD-BMP-7 ····· 19

3.6. Establishment of a biological interaction network based on differentially regulated mRNAs in HTMCs co-treated with steroid and mPTD-BMP-7 ····· 23

4. DISCUSSION ····· 26

5. CONCLUSION ····· 30

REFERENCES ····· 31

ABSTRACT IN KOREAN ····· 34

LIST OF FIGURES

<Fig 1> Effect of steroid on transforming growth factor beta (TGF-β) expression in rabbit trabecular meshwork (TM) cells ····· 11
<Fig 2> Effect of steroid and micellized protein transduction domain (PTD)-fused bone morphogenetic protein (BMP-7) polypeptide (mPTD-BMP-7) on the ECM in human trabecular meshwork cells (HTMCs) ····· 14
<Fig 3> Alterations in ECM components after steroid and mPTD-BMP-7 treatment in HTMCs by immunofluorescence staining ····· 17
<Fig 4> Effect of mPTD-BMP-7 on steroid-induced changes in TM cell size and ECM volume ··· ····· 18
<Fig 5> Gene expression analysis of HTMCs treated with Steroid and mPTD-BMP-7 ····· 21
<Fig 6> Protein-protein interaction network of DEGs ····· 25

LIST OF TABLES

<Table 1> Antibodies used for western blotting 6
<Table 2> Primers used in quantitative reverse transcriptase polymerase chain reaction (RT-qPCR) 7
<Table 3> Genes identified as upregulated or downregulated after steroid treatment based on RNA-sequencing 21

ABSTRACT

Effect of Bone Morphogenetic Protein-7 on Steroid-induced Extracellular Matrix Synthesis in Human Trabecular Meshwork Cells.

Purpose : Long-term steroid use, though essential for treating eye diseases, can lead to increased intraocular pressure (IOP) and potentially glaucoma. This study investigated the effect of bone morphogenetic protein-7 (BMP-7) on steroid-induced extracellular matrix (ECM) synthesis in human trabecular meshwork (TM) cells. We sought to explore the potential of BMP-7 as a protective agent against steroid-induced ECM accumulation in the TM.

Methods : Human trabecular meshwork cells (HTMCs) were treated with either steroids alone or a combination of steroids and BMP-7 to compare their effects on ECM production. BMP-7, known for its transforming growth factor (TGF)-β antagonistic properties, was administered using a micellized protein transduction domain (mPTD)-fused BMP-7 polypeptide to enhance activity. Gene expression analysis was conducted to identify specific genes involved in ECM regulation.

Results : The results demonstrated that BMP-7 effectively inhibited steroid-induced ECM accumulation in HTMCs. There was a significant reduction in ECM production in the steroid and BMP-7 co-treated group compared to the steroid-only group. Furthermore, several genes involved in ECM regulation were identified in the co-treatment, underscoring BMP-7's potential role in modulating ECM metabolism.

Conclusion : This study provides evidence that BMP-7 exerts protective, anti-fibrotic effects in HTMCs by inhibiting steroid-induced ECM synthesis. These findings suggest that BMP-7 could serve as a promising therapeutic target for preventing or treating steroid-induced glaucoma by maintaining normal aqueous humor outflow and preventing IOP elevation.

Key words : Steroid; Glaucoma; Trabecular Meshwork; Extracellular Matrix; Bone morphogenetic protein-7

1. Introduction

Steroids are commonly used in the pharmacological management of various ocular conditions. However, their use is associated with a significant risk of increased intraocular pressure (IOP), which can lead to the development of steroid-induced glaucoma.[1,2] This condition may result in optic nerve damage and irreversible vision loss. Despite this, the specific mechanisms underlying IOP elevation upon steroid administration remain unclear.[3,4] The degree of IOP elevation varies depending on the dose and method of administration, with notable differences observed among individuals, even when receiving equivalent doses. Notably, not all individuals exposed to steroids develop glaucoma, as the risk is influenced by genetic factors, steroid dosage, treatment duration, and baseline ocular conditions. Children are particularly susceptible to elevated IOP, necessitating vigilant monitoring and consideration of alternative therapies when possible. In severe cases, surgical intervention may be necessary to regulate IOP and preserve vision, highlighting the importance of weighing the therapeutic advantages of steroids against their potential adverse effects.[5] Therefore, identifying the etiology of steroid-induced glaucoma is crucial for ensuring the safe administration of steroids.

The most likely mechanism underlying steroid-induced elevation of IOP involves the activation of extracellular matrix (ECM) synthesis in the trabecular meshwork (TM), which is the primary route for aqueous humor outflow.[6,7] Previous studies have demonstrated increased levels of transforming growth factor beta (TGF-β) in the aqueous humor of individuals with steroid-induced glaucoma.[1,8-10] Steroids can enhance the expression of TGF-β, which in turn accelerates the accumulation and restructuring of ECM components within the TM. Excess ECM obstructs pores in the TM that normally facilitate the drainage of aqueous humor into the venous system, leading to compromised drainage and increased IOP.[6] Prolonged IOP elevation can lead to optic nerve damage, culminating in the development of glaucoma.

Bone morphogenetic protein-7 (BMP-7), a member of the TGF-β superfamily, is known for its role in the development of bone and cartilage, as well as its regenerative properties in various tissues. BMP-7 functions by antagonizing the effects of TGF-β by inhibiting TGF-β-associated signaling pathways.[11] This inhibition is expected to prevent excessive deposition and remodeling of the ECM, which contribute to elevated IOP in steroid-induced glaucoma. Owing to its antagonistic relationship with TGF-β, BMP-7 emerges as a promising therapeutic candidate, with the potential to alleviate fibrotic changes in the TM, thereby facilitating proper aqueous humor outflow and potentially preventing the onset of glaucoma.

Given that TGF-β is involved in steroid-induced ECM accumulation and that BMP-7 inhibits TGF-β, we explored the potential of BMP-7 in preventing steroid-induced ECM accumulation. To enhance the activity of BMP-7, we utilized a micellized protein transduction domain (PTD)-fused BMP-7 polypeptide (mPTD-BMP-7). This modified form of BMP-7 is designed to penetrate cells more efficiently and exert a stronger inhibitory effect on TGF-β signaling. [12-14] This study aimed to investigate the proteins affected by steroids and BMP-7 and their impact on human TM cells (HTMCs), and to identify associated gene expression changes through RNA-sequencing.

2. MATERIALS AND METHODS

2.1. Animals

All animal experiments were conducted in accordance with the guidelines and regulations for experimental ethics and were approved by the Institutional Animal Care and Use Committee of Korea Conformity Laboratories. Specific pathogen-free New Zealand White Rabbits (Samtakobio Korea, Gyeonggi, Korea) were used for in vivo pharmacokinetic analysis and safety assessment. The animals were housed under controlled conditions (temperature, 20–26°C; humidity, 40–60%). A total of 12 New Zealand White rabbits, each weighing between 2.5 and 3 kg, were used in this study, in compliance with the guidelines set by the Association for Research in Vision and Ophthalmology. Approval was obtained from the institutional animal ethics committee.

2.2. mPTD-BMP-7 preparation

The bacterial exepression vector for PTD-BMP-7 and protein purification have been described previously. [12-16] This PTD fusion peptide enables the direct transduction of proteins across the cell membrane. The denatured polypeptide was micellized with filtered 0.1% egg lecithin (BOC Sciences, Shirley, NY, USA) using sonication

2.3. Steroid and mPTD-BMP-7 treatment of rabbits

The rabbits were divided into three groups, with four rabbits in each group. The right eye of each rabbit was injected, while the left eye remained untreated. The control group received balanced salt solution (BSS), the second group received dexamethasone (5 mg/mL) injections, and the third group received a combination of dexamethasone and mPTD-BMP-7 (20 ng/mL). The rabbits were anesthetized by intramuscular administration of alfaxalone (3–5 mg/kg), followed by local anesthesia using 0.5% proparacaine hydrochloride eye drops. The injections were delivered through three routes into the eye: 0.05 mL into the anterior chamber, 0.05 mL into the vitreous cavity, and 0.2 mL into the subconjunctival space, using a 30-gauge needle syringe. The injections were administered weekly for four weeks, followed by a four-week observation period without additional treatment. After eight weeks, the rabbits were sacrificed, and their eyes were collected for

histological analysis.

2.4. Histological examination

After sacrificing the animals, the eyeballs were promptly removed and cut into small 1 mm^3 clumps. The samples were fixed by immersion in 2.5% glutaraldehyde (16220; Electron Microscopy Sciences) diluted in 0.1 M phosphate buffer for 2 h at room temperature. Samples were rinsed twice with 0.1 M phosphate buffer and post-fixed with 1% osmium tetroxide (75632; Sigma-Aldrich) diluted in 0.1 M phosphate buffer for 1 h at 4°C. Next, the samples were dehydrated with a series of graded ethyl alcohol solutions (100983; Merck Millipore) and then with acetone (A18-4; Fisher Scientific). The samples were then embedded in EPON 812. Ultrathin sections (70–80 nm) were obtained using an ultramicrotome (Leica Ultracut UCT, Leica, Wetzlar, Germany), stained with uranyl acetate (NC1375332; Fisher Scientific) and lead citrate (NC1588038; Fisher Scientific), and examined using a transmission electron microscope (JEM-1010; JEOL, Tokyo, Japan) at 60 kV. Sections from each eye, extending from the corneal apex to the optic nerve plane, were subjected to Masson's trichrome staining to assess collagen expression. Images were captured using a Leica DM4 microscope (DM400B; Leica, Wetzlar, Germany) and analyzed using the ImageJ software. Changes in TM cells were quantified by measuring the red-stained area, while TM cell size was calculated as the percentage of red-stained tissue within the total area. ECM expression was quantified by CVF, calculated as the percentage of the blue-stained tissue area within the total area.

2.5. Isolation and culture of HTMCs

Primary HTMCs were purchased from Sciencell (6950) and utilized for experiments at passages 3–6. The HTMCs were cultured in TM Cell Medium (TMCM) from Sciencell (6951). All cultures were maintained in a controlled environment with 5% CO_2 and 95% air at 37°C.

2.6. Treating HTMCs with steroids and mPTD-BMP-7

Two sets of experiments were conducted to investigate ECM mechanics following dexamethasone treatment in HTMCs. In the first experiment, ECM mechanics were observed after treatment with dexamethasone alone, while in the second experiment, ECM mechanics were evaluated over time after treatment with both dexamethasone and mPTD-BMP-7. To assess the

effect of dexamethasone on HTMCs, cells were cultured in 6-well plates (5,000–10,000 per cm^2) with 2 mL of culture medium per well. One group served as the untreated control, while the other two groups were treated with 100 nM dexamethasone (1.6 μL per well) for 1, 2, 3, and 7 days. Additionally, the last group was treated under the same conditions as the dexamethasone-treated groups but received an additional 20 ng/mL mPTD-BMP-7 (1 μL per well) along with dexamethasone. In summary, primary HTMCs were treated with control, dexamethasone, or dexamethasone + mPTD-BMP-7 in TMCM for 1, 2, 3, and 7 days.

2.7. Imaging the ECM

To identify F-actin and fibronectin in the cytoplasm of HTMCs, both test and control cells were cultured on 24-well plates with coverslips. Cells were fixed with 4% formaldehyde and permeabilized with 0.1% Triton X-100. After blocking with 1% bovine serum albumin, cells were incubated with primary antibodies diluted in blocking buffer at 4°C overnight, followed by incubation with fluorochrome-conjugated secondary antibodies. Fluorescence was visualized using a confocal microscope (LSM 700; Zeiss). The reagents used for immunofluorescence are as follows: Alexa Fluor 488 phalloidin (1:1000 dilution; A12379; Thermo Fisher) and fibronectin (1:250 dilution; sc-8422; Santa Cruz Biotechnology,).

2.8. Protein extraction and western blot analysis

Following dexamethasone and mPTD-BMP-7 treatment, cells were lysed at the end of each time point (Day 3 and 7), and proteins were isolated for western blotting. Cells were washed with cold 1x phosphate-buffered saline (PBS) and harvested by centrifugation at 1,000 rpm for 5 min. The cell pellet was collected and lysed with 50 μL RIPA Buffer (Biosesang, Korea) for protein extraction. After centrifugation at 15,000 rpm for 20 min, the lysates were transferred to a new microcentrifuge tube for protein quantification using the BCA assay (Thermo Fisher, USA). Equal amounts of protein were mixed with 5x sample buffer (ELPIS, Korea) and boiling at 100°C for 10 min. The samples were then loaded onto an 8% sodium dodecyl sulfate-polyacrylamide gel for electrophoresis, and the proteins were transferred onto a polyvinylidene difluoride membrane (Millipore, USA).

The membrane was blocked with 5% skim milk for 1 h and incubated with the primary antibodies overnight at 4°C. After three washes with 1x TBST, the membrane was incubated with secondary antibody for 1 h. After three washes with 1x TBST, the protein bands were visualized using an

enhanced chemiluminescence detection reagent (Bio-Rad, USA). The antibodies used for western blotting are listed in Table 1.

Alterations in ECM structure correlated with changes in protein expression, as confirmed by western blotting. The experiment was repeated three times, and ImageJ software was used for protein quantification.

Table 1. Antibodies used for western blotting

Target protein	Company	Catalog number
Fibronectin	Santa Cruz Biotechnology	sc-8422
GAG	Abcam	ab100970
Collagen 1	Santa Cruz Biotechnology	sc-293182
α- SMA	Abcam	ab7817
TGF-β	Cell Signaling Technology	3711S
TGF-β 1	Proteintech	21898-1-AP
TGF-β 2	Proteintech	19999-1-AP
Alpha-Tubulin antibody	Sigma-Aldrich	T6199-100

2.9. RNA extraction and RT-qPCR

HTMCs were seeded in a 6-well culture dish at a density of 4×10^5 cells/well and cultured for 16 h. The cells were treated with dexamethasone and/or mPTD-BMP-7 as previously mentioned. After treatment, the cells were collected for RNA extraction. The supernatant was removed, and the cells were washed once with cold 1x PBS. TRI Reagent (Molecular Research Center, USA) was added to each well (500 μL per well), and the contents were transferred to a microcentrifuge tube. Then, 200 μL of chloroform (Daegung, Korea) was added to each tube. The mixture was vortexed and incubated at room temperature for 10 min, followed by centrifugation at 15,000 rpm for 10 min to separate the phases. The upper aqueous phase containing RNA was carefully transferred to a new tube, and an equal volume of isopropanol (Daegung, Korea) was added. Centrifugation was performed at 15,000 rpm for 10 min. The supernatant was discarded, and 500 μL of 70% ethanol (Millipore, USA) was added to wash the RNA pellet. After removing the supernatant, the samples were air-dried at room temperature for 30 min. The RNA was resuspended in RNase-free water and quantified.

Next, RT-qPCR was performed to compare mRNA expression levels. cDNA was synthesized using the RNA-to-cDNA EcoDry Premix (Oligo dT) from Takara Bio (USA). PCR was performed using the SYBR Premix Ex Taq (Takara) and the StepOnePlus Real-Time PCR system (Thermo Fisher Scientific, USA). The forward and reverse primers used are summarized in Table 2. Relative gene expression levels were determined using the comparative 2-ΔΔCT method.

Table 2. Primers used in quantitative reverse transcriptase polymerase chain reaction (RT-qPCR)

Gene	Sequence (5′ to 3′)	Primers
FIBRONECTIN	TGC GGC AGT TGT CAC AG	F
	CCG TGG GCA ACT CTG TC	R
GAG	AGG AAG TAC CTG CCC CTC AT	F
	CTC AGG ATT GGC GTT TTC AT	R
COLLAGEN 1	CATGTTCAGCTTTGTGGACCT	F
	GCAGCTGACTTCAGGGATGT	R
HBB	TGCGGGTCAAAGTGTACTTCC	F
	ACTGCACGTCTAGGTTGAGTC	R
ANKRD1	AGTAGAGGAACTGGTCACTGG	F
	TGTTTCTCGCTTTTCCACTGTT	R
HBA2	ACAAGCTTCGGGTGGACC	F
	ACGGTATTTGGAGGTCAGCA	R
ISY1-RAB43	TGGCAAGAGGAGAAAAGGAA	F
	GCCTCCTCAATCTCTTGCTG	R
VAMP8	TGTGCGGAACCTGCAAAGT	F
	CTTCTGCGATGTCGTCTTGAA	R
MAGED4B	CAGCAAGATGAGGGTCCTGA	F
	GCGCTTCATCCCCGATATTC	R
DOCK2	AGAAATGTCAAAAGACCAGCCA	F
	TATGACCGTTTGCTTGTTGGG	R
CD36	GGCTGTGACCGGAACTGTG	F
	AGGTCTCCAACTGGCATTAGAA	R

MCF2L	TGTTGTTATCGACAGACGAAGAG	F
	AAGCGAGATGGACGAAGGATG	R
GIP	AAGTGGACATGGACAAGCTCC	F
	CCTCCGACTTGAACACCTCC	R
IL34	CCTGGCTGCGCTATCTTGG	F
	AGTGTTTCATGTACTGAAGTCGG	R
S100A14	GAGACGCTGACCCCTTCTG	F
	CTTGGCCGCTTCTCCAATCA	R
SERPINB7	AAATGCAGAGTTTTGCTTCAACC	F
	GAAGAGTTTCCATATCCTGAGGC	R
SMIM11A (C21orf51)	AATTGGAAGGTCCTAACTGGGA	F
	CTTGTCGGCAAAGTGGTGG	R
GAPDH	CAACGGATTTGGTCGTATTGG	F
	GGCAACAATATCCACTTTACCAGAGT	R

2.10. RNA sequencing and analysis

RNA library preparation and sequencing were conducted by LAS Inc. (Gimpo, Korea; http://www.lascience.co.kr/) using the SMARTER Stranded Total RNA-seq kit-v2 – Pico Input Mammalian (Takara Bio, Mountain View, CA, USA) according to the manufacturer's instructions. This process included the ligation of RNAs with 3′ and 5′ adaptors, followed by reverse transcription to cDNA. PCR was performed with Illumina index primers to differentiate samples collected at various time points post-injury from both proximal and distal segments. Sequencing was carried out on a NextSeq 500 System (Illumina, San Diego, CA) with 75 bp paired-end reads.

Quality control was performed with FastQC v0.11.5, and sequencing adapters and low-quality bases were trimmed using Skewer v0.2.2. High-quality reads were aligned to the reference genome using STAR v2.6. Quantification of gene expression was achieved with Cuffquant in Cufflinks v2.2.1, and gene expression values were calculated as fragments per kilobase of transcript per million mapped reads (FPKM). Differential expression analysis among conditions (Control (serum-free) vs. Steroid, Steroid vs. Steroid with mPTD-BMP-7 treatment) was performed using Cuffdiff, identifying differentially expressed genes (DEGs) with a fold change cutoff of 2 and a p-value cutoff of 0.05. Unsupervised clustering of a selected subset of DEGs was conducted using R scripts. Scatter

plots, volcano plots, and comparisons between sample expression profiles were generated.

Functional enrichment analysis was performed using g:Profiler2 version 0.2.0 to investigate the biological roles of DEGs based on Gene Ontology (GO), KEGG, and other functional enrichment tools. Initially, 30 DEGs were selected from Table 3, to which an additional seven DEGs were added based on a broader fold change range, resulting in a total of 37 DEGs used for STRING analysis. Furthermore, 20 additional genes closely associated with these DEGs were integrated, enabling a comprehensive network analysis. This analysis identified 20 new interactions, providing insight into the intricate relationships between proteins and their roles in gene regulation.

2.11. Statistical analysis

All data are presented as the mean ± standard deviation. Differences between groups were examined via the Student's t-test and one-way analysis of variance using the SPSS statistical software (version 26.0; IBM Corp., Armonk, NY, USA). Values of $P < 0.05$ were considered statistically significant.

3. RESULTS

3.1. Effects of steroid and mPTD-BMP-7 on TGF-β levels in rabbit aqueous humor and TM tissue

To validate the prevailing theory that the concentration of TGF-β in aqueous humor increases during steroid treatment, the aqueous humor of rabbits administered dexamethasone, a steroid, with or without mPTD-BMP-7, was examined. The concentrations of TGF-β1 and TGF-β2 in aqueous humor were measured via western blotting. TGF-β1 concentration exhibited an approximately 2-fold increase compared to that in the control group, while TGF-β2 concentration showed a 6-fold increase (Fig. 1A). ECM levels are elevated in the TM of patients with steroid-induced glaucoma. To confirm this finding, we examined histological alterations using TEM. The results showed that the size of steroid-treated TM cells increased, and the extracellular space became significantly denser (Fig. 1B).

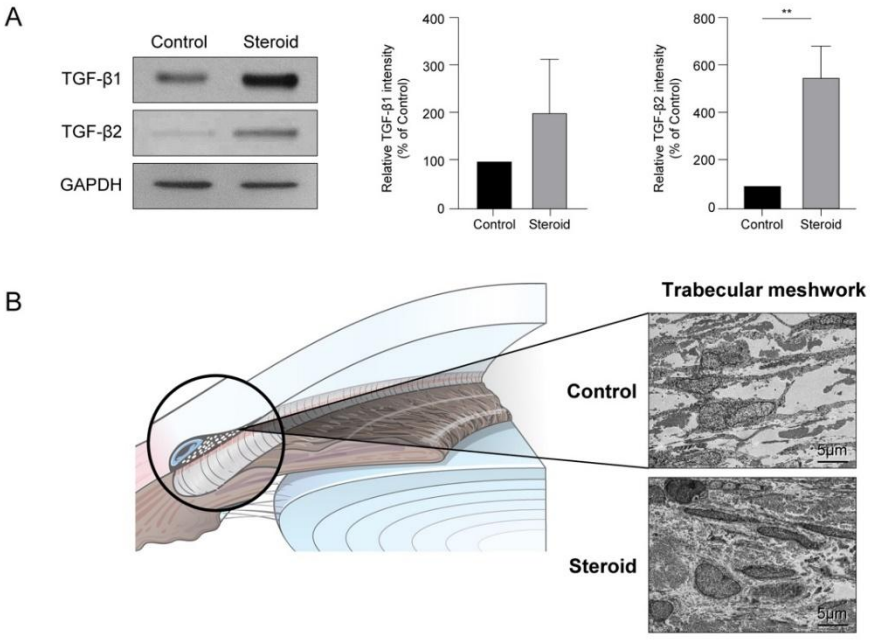

Figure 1. | Effect of steroid on transforming growth factor beta (TGF-β) expression in rabbit trabecular meshwork (TM) cells A. The expression level of TGF-β1 and TGF-β2 in rabbit aqueous humor before and after dexamethasone administration was assessed via western blotting. Both TGF-β1 and TGF-β2 expression increased in response to dexamethasone. Quantification of the protein bands showed that the increase in TGF-β2 expression was greater than that in TGF-β1. **B**. Comparison of histological alterations in the TM cells and extracellular matrix (ECM) after dexamethasone injection into the rabbit eye, as observed via transmission electron microscopy (TEM) (Scale bar: 5 μm, Magnification: 8000x). An increase in the size of TM cells was observed, accompanied by a denser ECM structure. (*, **, and *** indicate $P < 0.05$, $P < 0.01$, and $P < 0.001$, respectively)

3.2. Impact of steroid and mPTD-BMP-7 treatment on the ECM of HTMCs

We evaluated the mRNA expression of ECM components (collagen I, glycosaminoglycans [GAGs], and fibronectin) in HTMC upon steroid treatment via quantitative reverse transcriptase polymerase chain reaction (RT-qPCR). On Day 2, there was a significant increase in fibronectin expression in the cells treated with a dexamethasone when compared to that in the control and combination treatment (mPTD-BMP-7) groups. By Day 3, fibronectin levels remained high in the dexamethasone group but decreased in the combination treatment group. The expression of GAGs showed a similar pattern (Fig. 2A). Western blotting of the same samples indicated that dexamethasone alone led to an increase in the expression of α-smooth muscle actin (α-SMA), collagen I, GAGs, fibronectin, TGF-β1, and TGF-β2 over time, reaching a peak at Day 7. Combination treatment notably decreased the expression of these proteins compared to dexamethasone treatment alone, indicating that mPTD-BMP-7 alleviated the dexamethasone-induced upregulation of ECM components. Tubulin levels remained consistent across all groups and served as a loading control (Fig. 2B).

In the dexamethasone-treated group, fibronectin and collagen I increased over time, with significant increases observed on Day 7. In contrast, the combination of BMP-7 and steroid treatment effectively diminished the ECM, as evidenced by the reduced levels of fibronectin and collagen I by Day 7, which approached those in the control group. This finding suggests that BMP-7 may counteract steroid-induced ECM accumulation. TGF-β1 exhibited a modest increase

following steroid treatment; however, no significant response was noted when BMP-7 was co-administered. In contrast, TGF-β2 levels showed a marked increase on Day 7 following steroid treatment, while the combination of BMP-7 and steroid treatment significantly decreased TGF-β2 expression by Day 7, indicating a pronounced regulatory effect of BMP-7 (Fig. 2C).

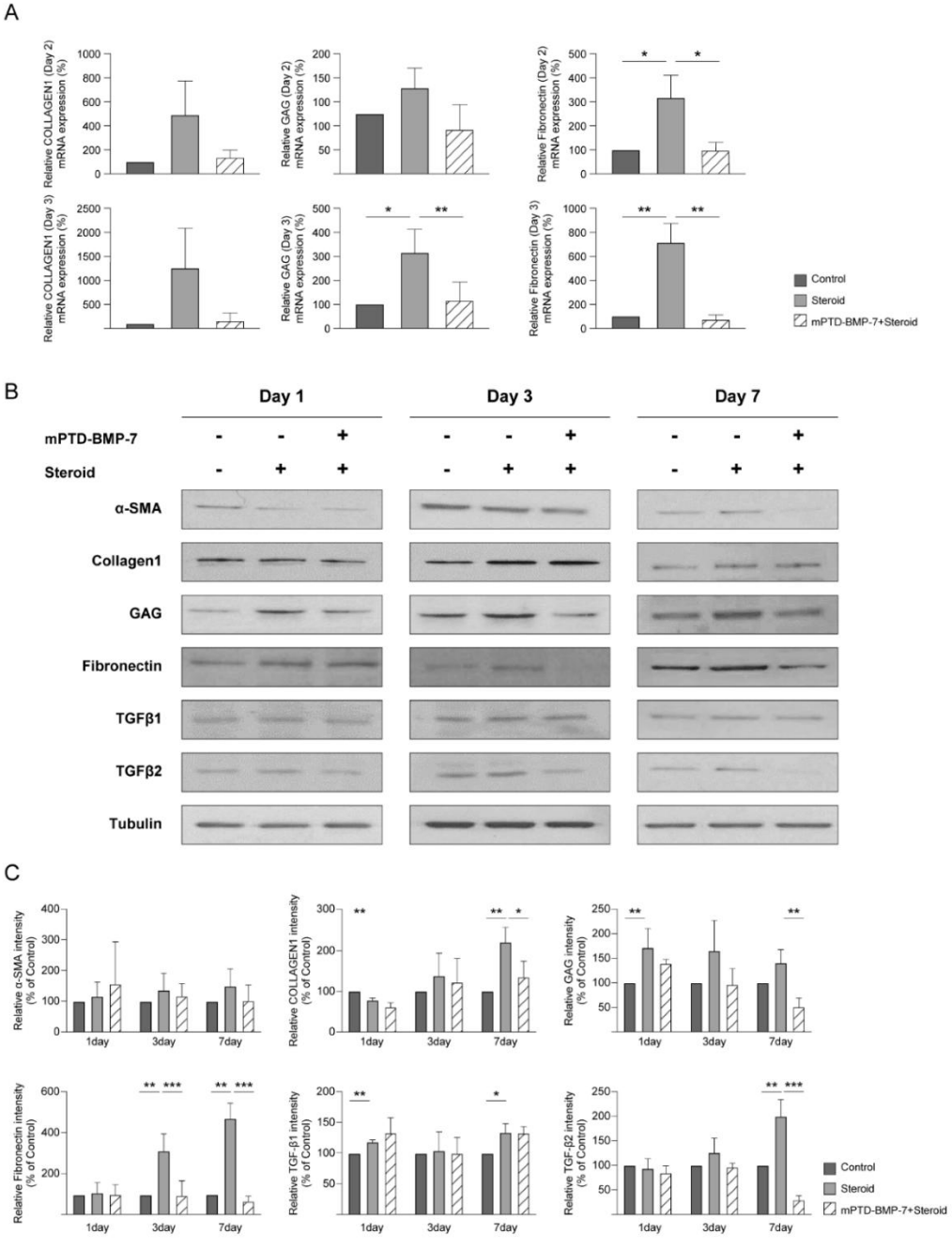

Figure. 2 | Effect of steroid and micellized protein transduction domain (PTD)-fused bone morphogenetic protein (BMP-7) polypeptide (mPTD-BMP-7) on the ECM in human trabecular meshwork cells (HTMCs) A. Quantitative reverse transcriptase polymerase chain reaction (RT-qPCR) for collagen I, GAGs, and fibronectin in HTMCs treated with 100 nM dexamethasone, with or without 20 ng/mL mPTD-BMP-7. mRNA expression levels in HTMCs on Day 2 (upper panels) and Day 3 (lower panels) of treatment. The baseline indicates the HTMCs that are not exposed to dexamethasone or mPTD-BMP-7. The relative collagen I, GAG, and fibronectin mRNA expression levels significantly decreased after 3 days of dexamethasone treatment (compared to the controls and after 2 days). This decrease was suppressed by mPTD-BMP-7 addition. **B.** and **C.** Western blotting for α-smooth muscle actin (α-SMA), collagen I, GAGs, fibronectin, TGF-β1, and TGF-β2 (tubulin was used as the loading control) in HTMCs over the course of 7 days. The representative bands for these proteins on Days 1, 3, and 7 are shown in **B.** and their quantification is shown in **C.** Collagen I, fibronectin, and TGF-β2 were upregulated in HTMCs exposed to dexamethasone on Day 7, while collagen I, GAGs, fibronectin, and TGF-β2 were downregulated in HTMCs exposed to dexamethasone along with mPTD-BMP-7. (*, **, and *** indicate $P < 0.05$, $P < 0.01$, and $P < 0.001$, respectively)

3.3. Alterations in ECM volume upon steroid and mPTD-BMP-7 co-treatment in HTMCs

We investigated alterations in ECM volume through imaging techniques, focusing on fibronectin, which showed significant variations in prior western blot analyses, and F-actin, which forms the structural framework of the ECM. Immunofluorescence staining was utilized to visualize changes in F-actin and fibronectin within HTMCs before and after dexamethasone administration. DAPI (blue) was utilized to visualize the nucleus, thereby indicating cell positioning and density. The F-actin that constitutes the cytoskeleton is shown in green, while red denotes Fibronectin, an ECM protein. The merged staining images provide a comprehensive overview of the structural organization and protein distribution within the cells (Fig. 3A).

In an additional experiment, alterations in ECM volume within HTMCs were investigated

following varying durations of exposure to BMP-7. Five distinct groups were analyzed: a control group (which received no exposure to steroids or BMP-7), a steroid-only group, and three groups that were treated with steroids in conjunction with BMP-7 exposure for different time intervals (1, 2, or 6 h). The levels of DAPI, F-actin, and fibronectin were compared across these groups. The control group exhibited the baseline distribution of F-actin and fibronectin, whereas the steroid-only group demonstrated a significant increase in the levels of both proteins. Conversely, the groups that were initially exposed to BMP-7 showed a progressive decline in F-actin and fibronectin levels, with the reductions becoming increasingly pronounced with the duration of BMP-7 exposure. The most substantial decrease was noted in the group subjected to BMP-7 for 6 h. The composite images presented in the bottom row illustrate the correlation between duration of BMP-7 exposure and the degree of ECM remodeling observed throughout the week (Fig. 3B)

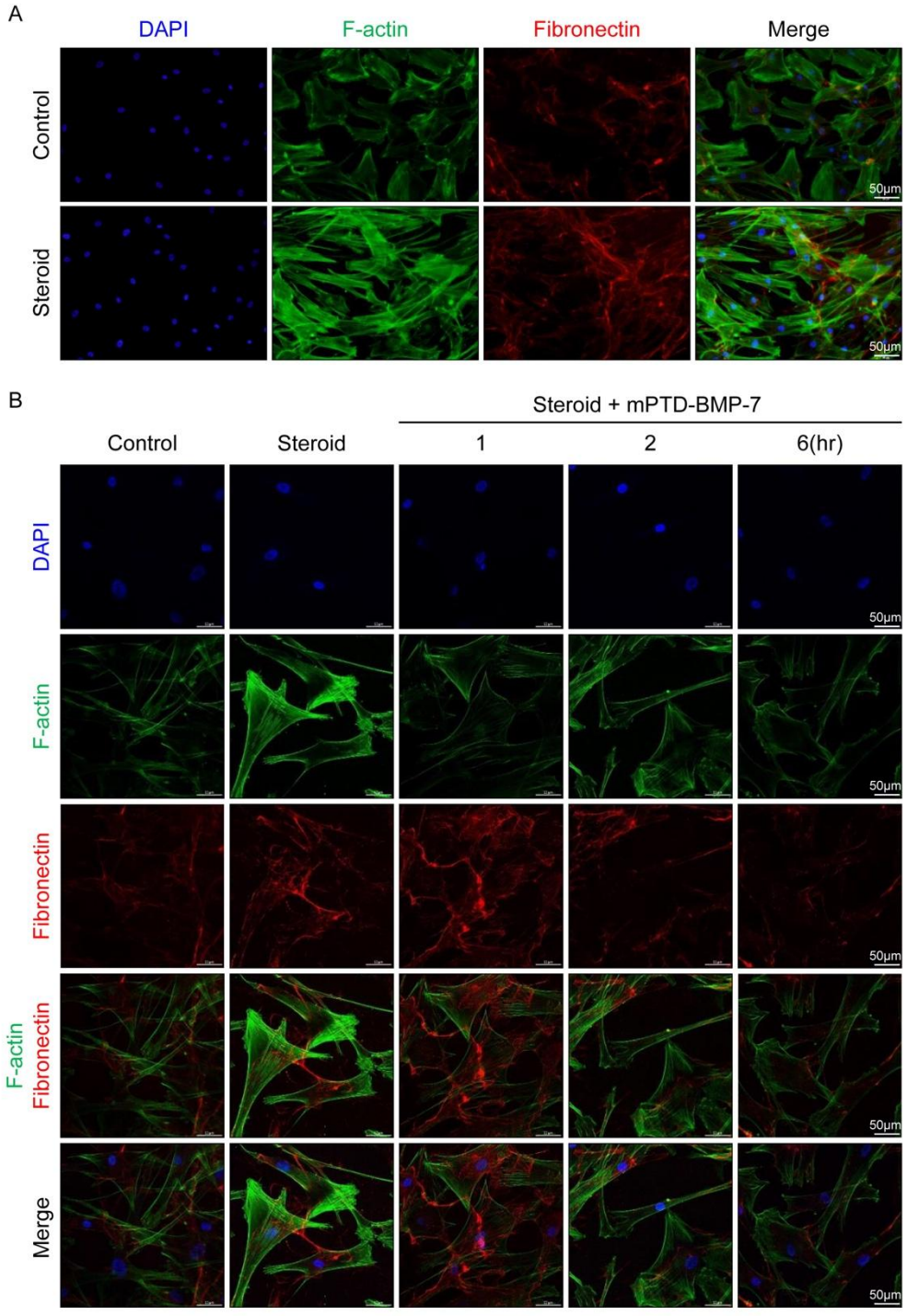

Figure. 3 | Alterations in ECM components after steroid and mPTD-BMP-7 treatment in HTMCs by immunofluorescence staining A. Immunofluorescence detection of F-actin and fibronectin in HTMCs. The first row shows cells that were not treated with dexamethasone (control group). The second row shows cells treated with dexamethasone. Cells stained with the nuclear stain DAPI are shown in the first column, those stained with F-actin are in the second column, fibronectin staining is shown in the third column, and a merge of all three is shown in the last column (DAPI + F-actin + fibronectin). **B.** The first row shows cells stained with DAPI, the second shows F-actin, the third shows fibronectin, the fourth shows F-actin and fibronectin, and the last row shows a merge of all three. The first column represents no treatment (control), the second indicates cells immediately after dexamethasone and mPTD-BMP-7 co-treatment, and the other three columns represent 1, 2, and 6 h after co-treatment, respectively. Confocal microscopy images (scale bar: 50 μm, magnification: 400x) reveal that fibronectin levels, which increased with steroid treatment alone, gradually decreased over time following co-treatment with mPTD-BMP-7.

3.4. Effect of steroid and mPTD-BMP-7 co-treatment on rabbit TM

In the control group, the cytoplasm of TM cells (stained red) and connective tissue (stained blue) reflected intact structures within TM tissue. However, in the steroid-treated group, there was a noticeable increase in the cytoplasmic area, indicating an increase in cell size, and substantial accumulation of connective tissue, suggesting an increase in the ECM. In the combination-treated group, the cytoplasmic area was reduced relative to the steroid-treated group, indicating that the increase in cell size was inhibited, and the amount of connective tissue was also reduced, reflecting decreased ECM accumulation. Quantitative analysis showed that cell size significantly increased in the steroid-only group but returned to levels similar to those of the control group in the combination-treated group. ECM quantification revealed a significant increase in ECM in the steroid-treated group, which was reduced to control levels in the combination-treated group. The result was quantified as connective tissue volume fraction (CVF) (Fig. 4)

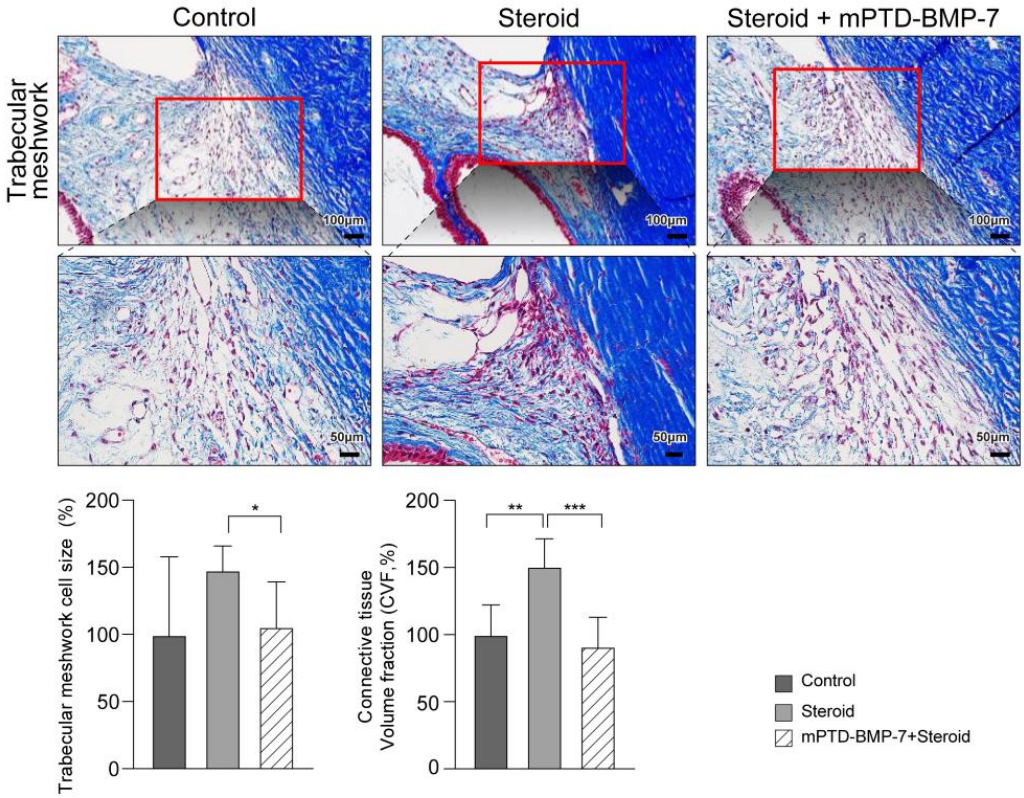

Figure 4. | Effect of mPTD-BMP-7 on steroid-induced changes in TM cell size and ECM volume Masson's trichrome staining of the TM in rabbits treated with dexamethasone (5 mg/mL) and mPTD-BMP-7 (20 ng/mL). Images were captured using a light microscope (Upper row: Scale bar: 100 μm, Magnification: 200x. Lower row: Scale bar: 50 μm, Magnification: 400x; the lower row images are magnified 2x from the upper row). Treatment with steroid alone leads to increased cell size and connective tissue volume within the TM, whereas co-treatment with mPTD-BMP-7 significantly mitigated these effects, restoring normal cell size and connective tissue volume. The data below confirm the quantitative analysis of changes observed in the images. (*, **, and *** indicate $P < 0.05$, $P < 0.01$, and $P < 0.001$, respectively)

3.5. Identification of differential mRNA expression in HTMCs treated with steroid and mPTD-BMP-7

The volcano plot (Fig. 5A) highlights genes with statistically significant fold changes between the steroid-only and steroid combined with BMP-7 treatment groups, while the heat map (Fig. 5B) visualizes the clustering of gene expression patterns across samples, emphasizing the distinct regulatory effects of these treatments. Pathway enrichment analysis was performed using Ingenuity Pathway Analysis (IPA) and KEGG databases, revealing enriched biological processes and pathways (Benjamini-Hochberg FDR < 0.05). GO analysis (Fig. 5C) further highlighted significant terms, and the largest clusters were enriched with genes related to the regulation of cell death and nitric oxide (NO) transport.

Fourteen genes associated with related biological processes, identified through GO analysis (in Fig 5C), were selected for RT-qPCR validation. Among these, three genes—SERPINB7, SMIN11A, and Relative GIP—exhibited significant changes specifically when steroid and BMP7 were administered together. Notably, four genes—ISY1-RAB43, VAMP8, DOCK2, and MAGED4B—demonstrated consistent and significant alterations in expression across both the steroid-only and steroid + BMP7 treatment groups, highlighting their potential key roles in response to both treatments (Fig 5D).

In addition to the genetic alterations observed following co-treatment with steroids and BMP-7, genes that were predominantly affected by steroids only were categorized separately. Upon administration of steroids to HTMCs, 14 genes exhibited upregulation while 16 genes were downregulated (Table 3).

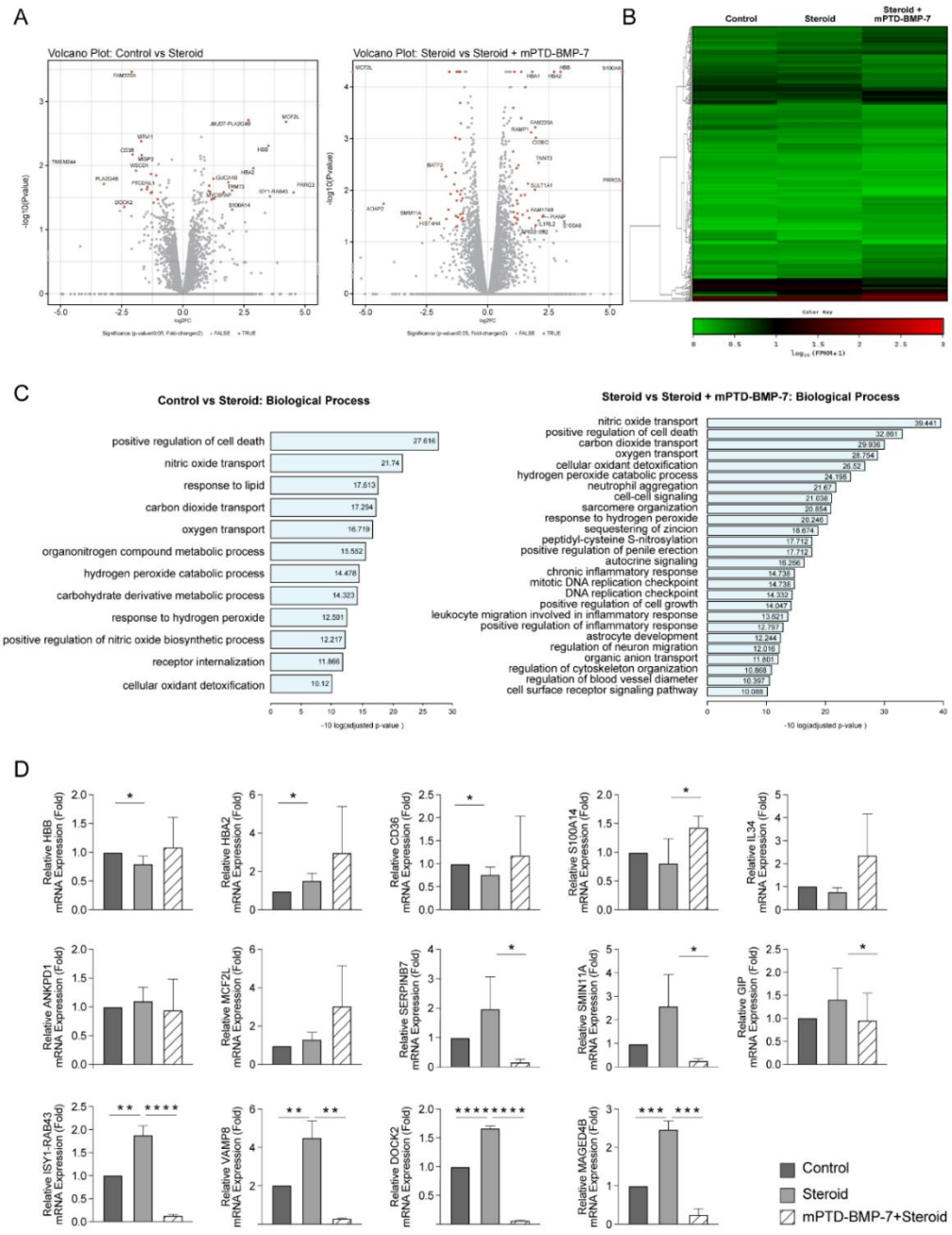

Figure 5. | Gene expression analysis of HTMCs treated with dexamethasone and mPTD-BMP-7

A. Volcano plots with $\log_2$ fold-change ($\log_2$fc) versus $-\log_{10}$ (P-value) representing the change in gene expression and its significance. These plots illustrate differential RNA expression between the control and dexamethasone-treated group (left plot) as well as between the dexamethasone-treated and dexamethasone + mPTD-BMP-7-treated group (right plot). **B.** Heatmap illustrating relative RNA expression in the control, dexamethasone, and dexamethasone + mPTD-BMP-7-treated groups. **C** Gene Ontology (GO) analysis was conducted to identify the significantly enriched biological processes in the comparisons between the control versus dexamethasone and dexamethasone versus dexamethasone + mPTD-BMP-7. **D.** RT-qPCR confirmation and comparison of RNA-sequencing results. The genes that showed the greatest change before and after dexamethasone + mPTD-BMP-7 treatment were VAMP8, DOCK2, ISY-1-RAB43, and MAGED4B, listed in the bottom row. (*, **, and *** indicate $P < 0.05$, $P < 0.01$, and $P < 0.001$, respectively)

Table 3. Genes identified as upregulated or downregulated after steroid treatment based on RNA-sequencing

Up-regulated Gene name	Log_2 (Fold-change)	P-value	Full descriptions of the gene
MAGED4B	4.504	0.026	MAGE family member D4B [Source Symbol;Acc:HGNC:22880]
MCF2L	4.196	0.002	MCF.2 cell line derived transforming sequence like [Source Symbol;Acc:HGNC:14576]
ISY1-RAB43	3.541	0.030	ISY1-RAB43 readthrough [Source Symbol;Acc:HGNC:42969]
HBB	3.488	0.005	Hemoglobin subunit alpha 2 [Source Symbol;Acc:HGNC:4827]
HBA2	2.875	0.011	Hemoglobin subunit alpha 2 [Source Symbol;Acc:HGNC:4824]

JMJD7-PLA2G4B	2.666	0.002	JMJD7-PLA2G4B readthrough [Source Symbol;Acc:HGNC:34449]
TRIM73	1.993	0.025	Tripartite motif containing 73 [Source Symbol;Acc:HGNC:18162]
S100A14	1.992	0.049	S100 calcium binding protein A14 [Source Symbol;Acc:HGNC:18901]
GUCA1B	1.852	0.019	Guanylate cyclase activator 1B [Source Symbol;Acc:HGNC:4679]
MYCBPAP	1.658	0.026	MYCBP associated protein [Source Symbol;Acc:HGNC:19677]
VAMP8	1.291	0.033	Vesicle associated membrane protein 8 [Source Symbol;Acc:HGNC:12647]
PSG5	1.250	0.016	Pregnancy specific beta-1-glycoprotein 5 [Source Symbol;Acc:HGNC:9522]
TMEM121	1.207	0.033	Transmembrane protein 121 [Source Symbol;Acc:HGNC:20511]
AK9	1.151	0.034	Adenylate kinase 9 [Source Symbol;Acc:HGNC:33814]

Down-regulated Gene name	**Log_2(Fold-change)**	**P-value**	**Full descriptions of the gene**
PLA2G4B	-3.215	0.020	Phospholiapase A2 group IVB [Source: HGNC Symbol; Acc: HGNC:9036]
DOCK2	-2.382	0.044	Dedicator of cytokinesis 2 [Source: HGNC Symbol; Acc: HGNC:2988]
FAM220A	-2.095	0.000	Family with sequence similarity 220 member A [Source: HGNC Symbol; Acc: HGNC:22422]
CD36	-2.043	0.007	CD36 molecule [Source: HGNC Symbol; Acc: HGNC:1663]
WSCD1	-1.901	0.012	WSC domain containing 1 [Source: HGNC Symbol; Acc: HGNC:29060]

MRVI1	-1.702	0.004	Murine retrovirus integration site 1 homolog [Source: HGNC Symbol; Acc: HGNC:7237]
FTCDNL1	-1.687	0.024	Formiminotransferase cyclodeaminase N-terminal like [Source: HGNC Symbol; Acc: HGNC:48661]
MISP3	-1.676	0.007	MISP family member 3 [Source: HGNC Symbol; Acc: HGNC:26963]
IL34	-1.467	0.023	Interleukin 34 [Source: HGNC Symbol; Acc: HGNC:28529]
XKR6	-1.439	0.022	XK related 6 [Source: HGNC Symbol; Acc: HGNC:27806]
SERPINB7	-1.301	0.014	Serpin family B member 7 [Source: HGNC Symbol; Acc: HGNC:13902]
LTK	-1.296	0.027	Leukocyte receptor tyrosine kinase [Source: HGNC Symbol; Acc: HGNC:6721]
CATSPERE	-1.263	0.026	Catsper channel auxiliary subunit epsilon [Source: HGNC Symbol; Acc: HGNC:28491]
KRTAP2-3	-1.189	0.038	Keratin associated protein 2-3 [Source: HGNC Symbol; Acc: HGNC:18906]
ZC3H11B	-1.079	0.014	Zinc finger CCCH-type containing 11B [Source: HGNC Symbol; Acc: HGNC:29659]
RAMP1	-1.015	0.034	Receptor activity modifying protein 1 [Source: HGNC Symbol; Acc: HGNC:9843]

3.6. Establishment of a biological interaction network based on differentially regulated mRNAs in HTMCs co-treated with steroid and mPTD-BMP-7

Establishment of a biological interaction network based on differentially regulated mRNAs in HTMCs co-treated with steroid and mPTD-BMP-7

As shown in Fig. 5D, the expression of four genes was significantly upregulated or downregulated when treated with steroids alone or in combination with mPTD-BMP-7. Among these genes,

DOCK2 and VAMP8 were found to be associated with the same biological process network. Additionally, CD36, which was significantly downregulated after treatment with steroids alone, and SERPINB7, which was significantly downregulated after combination treatment with both steroids and mPTD-BMP-7, were interconnected within the same network (Fig. 6).

Using Cytoscape and its applications EnrichmentMap and AutoAnnotate, functional clustering was applied to the STRING-generated network, producing 37 distinct DEGs. STRING analysis allowed us to further explore how these genes interact within biological pathways and processes. The node color corresponds to the $\log_2$ fold change indicated as $\log_2$fc. This visual representation highlights the extent of changes in certain genes in response to steroid or combined treatment, emphasizing the functional impact of these treatments on key biological processes.

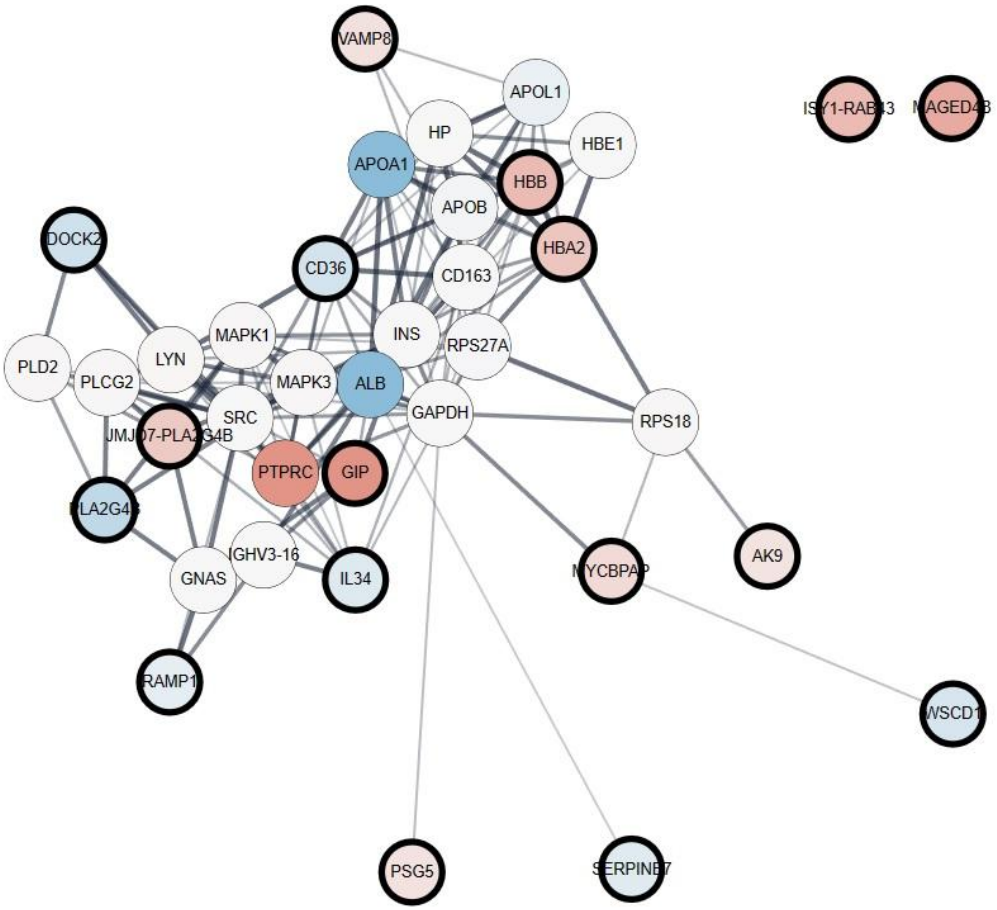

Figure. 6 | Protein-protein interaction network of DEGs A protein-protein interaction (PPI) network was constructed using STRING software to visualize the relationships among the 37 differentially expressed genes (DEGs) identified in this study. This analysis allowed for the identification of additional interactions, revealing how these genes collaborate within biological pathways. Among the four genes that demonstrated significance in the RT-qPCR results of Fig. 5-D, DOCK2 and VAMP8 exhibited direct connections within this network, indicating their potential key roles in the underlying biological processes. In contrast, ISY1-RAB43 and MAGED4B did not show direct interactions with the other DEGs, suggesting a more isolated functional role.

4. DISCUSSION

The ECM plays a crucial role in the structure and function of HTMCs, which are essential for regulating IOP by controlling the outflow of the aqueous humor from the eye.[5] The TM is a complex structure composed of beams and sheets of connective tissue, where ECM components, such as collagen, elastin, fibronectin, F-actin, and GAGs, provide structural support, regulate cell behavior, and modulate aqueous humor flow.[17] GAGs are long, unbranched polysaccharides that contribute to the viscoelastic properties of the ECM and regulate cell signaling. Collagen forms a scaffold that provides tensile strength and maintains the structural integrity of the TM. Glycoproteins such as fibronectin mediate cell adhesion and migration by interacting with other ECM components and cell surface receptors, while F-actin, a polymerized form of actin, is a key component of the cytoskeleton that interacts with ECM proteins at cell-ECM junctions. Understanding how these ECM components respond to steroids and mPTD-BMP-7 is crucial for developing therapeutic strategies to manage ocular disorders, such as glaucoma, where dysregulation of ECM turnover can impair aqueous humor outflow and elevate IOP.[18]

In this study, significant changes in the ECM were observed at both the mRNA and protein levels in HTMCs. Notably, fibronectin exhibited substantial alterations at the genetic level, with mRNA expression patterns showing more pronounced differences on Day 3 of treatment compared to Day 2. These differences suggest a time-dependent effect of the treatments on fibronectin production (Fig. 2A). At the protein level, changes in the ECM and TGF-β were observed, with the most dramatic changes occurring on Day 7. Specifically, there was a significant increase in fibronectin and TGF-β2 levels when treated with steroid alone, whereas a notable decrease was observed when mPTD-BMP-7 was added. These findings highlight the potential role of mPTD-BMP-7 in modulating the effects of steroids on ECM protein synthesis. The pronounced changes in fibronectin and TGF-β2 expression on Day 7 suggest that these effects became most significant over time, indicating a cumulative impact of the treatments (Fig. 2B, C).

Fibronectin was the ECM component that showed the most significant increase in response to steroid treatment, accompanied by a notable rise in F-actin levels, consistent with previous studies.[19,20] This increase suggests potential densification of the extracellular space, with implications for cellular function and tissue structure (Fig. 3A). The dynamic nature of ECM remodeling was further evidenced by the time-dependent changes observed following treatment with

steroids and mPTD-BMP-7. A rapid decrease in fibronectin and F-actin levels occurred after treatment, with both returning to baseline levels by 6 h (Fig. 3B). These findings indicate a significant reduction in ECM density after treatment, suggesting that the combination of steroids and mPTD-BMP-7 induces dynamic ECM changes that may influence tissue function.

TGF-β and BMP-7, both members of the TGF-β superfamily, play crucial roles in various cellular processes, including tissue development, homeostasis, and fibrosis. Under normal conditions, TGF-β and BMP-7 signaling pathways interact and counterbalance each other to maintain tissue homeostasis. However, in fibrosis, this balance can be disrupted, leading to aberrant signaling that contributes to the pathological process. TGF-β is well-known for its pro-fibrotic effects, promoting the production of ECM components and stimulating fibroblast activation, which can lead to excessive tissue scarring.[9,21,22] In contrast, BMP-7 has been shown to have anti-fibrotic properties, counteracting the effects of TGF-β and promoting tissue regeneration and repair. Dysregulation in the balance between TGF-β and BMP-7 signaling, such as decreased BMP-7 levels or increased TGF-β signaling, can enhance fibrosis by promoting fibroblast activation, collagen deposition, and tissue remodeling.

SMAD proteins are intracellular signaling molecules that transmit signals from TGF-β family ligands from the cell surface to the nucleus, regulating gene expression.[10,23] TGF-β and BMP-7 influence SMAD signaling in similar yet distinct ways: TGF-β primarily activates Smad2 and Smad3, while BMP-7 predominantly activates Smad1, Smad5, and Smad8.[24] Although the exact mechanism through which BMP-7 acts in HTMCs is not fully understood, it is thought that BMP-7 and TGF-β act within the same SMAD signaling pathway but at different steps. This difference may allow BMP-7 to selectively inhibit ECM production without disrupting TGF-β's normal immune-regulatory functions.

Fuchshofer et al. observed changes in ECM-related factors after administering BMP-7 and TGF-β2 together to HTMC.[11] When TGF-β2 was administered alone, there was an increase in CTGF, TSP-1, fibronectin, collagen types IV and VI, and PAI-1, which are ECM components. However, when TGF-β2 and BMP-7 were co-administered, the increase in these components was suppressed. No effects were observed when BMP-7 was administered alone. This confirmed that BMP-7 acts as an antagonist to TGF-β2. However, this study diverges from previous research in several key aspects. Whereas prior studies focused primarily on the antagonistic relationship between BMP-7 and TGF-β, our investigation centered on BMP-7's role in reducing the ECM accumulation increased by

steroids. We aimed to explore the potential of BMP-7 as a treatment for steroid-induced glaucoma by examining its ability to counteract the increase in TGF-β2 triggered by steroid treatment. It is important to note that while BMP-7 shows promise in preclinical studies, its efficacy and safety as a treatment for glaucoma, including steroid-induced glaucoma, have not been conclusively established in human clinical trials. BMP-7 has been studied for its potential to attenuate fibrosis not only in the TM but also in other tissues, such as the kidneys, pancreas, and liver. Studies using mPTD-BMP-7 have demonstrated its increased efficacy in delivering BMP-7's therapeutic effects to these tissues.[15,16,25-27] These findings suggest that mPTD-BMP-7, with its superior delivery and activity, may be a viable therapeutic agent across multiple clinical indications.

Gene expression analysis was conducted to elucidate the mechanism through which BMP-7 inhibits ECM production and TGF-β activity in HTMCs. A notable finding was the differential mRNA expression levels observed when steroids were administered alone versus in combination with mPTD-BMP-7. Specifically, the expression of genes, such as VAMP8, DOCK2, ISY1 splicing factor homolog readthrough (ISY1-RAB43), and melanoma-associated antigen D4B (MAGED4B), increased with steroid treatment alone but decreased when steroids were combined with mPTD-BMP-7 (Fig. 5D). VAMP8, primarily known for its role in vesicle trafficking and exocytosis, likely influences ECM remodeling by regulating the secretion of ECM components and remodeling enzymes.[25,28] DOCK2, although traditionally associated with immune cell migration and cytoskeletal reorganization, may intersect with BMP-7 signaling pathways, thereby affecting ECM production in TM cells.[29,30] ISY1-RAB43, involved in intracellular vesicle trafficking, is hypothesized to affect cell size rather than directly influencing ECM synthesis, potentially altering secretion dynamics and cellular morphology.[31,32] Lastly, MAGED4B, despite being less studied in ECM regulation, may modulate ECM synthesis through its effects on cellular signaling and gene expression, possibly interacting with established ECM-related pathways such as TGF-β signaling.[33,34] Collectively, these genes may play significant roles in ECM regulation, thereby necessitating further investigation into their precise mechanisms.

The most significant genes were validated through RT-qPCR analysis and included VAMP8, DOCK2, ISY1-RAB43, and MAGED4B. Given that VAMP8 and DOCK2 act within the same network (Fig. 6), it is likely that these are related to effects of steroids and BMP-7.[35,36] The biological processes that showed significant changes following the administration of steroids and BMP-7 were related to NO, carbon dioxide (CO_2), and oxygen transport (Fig. 5C).

NO is a signaling molecule that plays diverse roles in cellular physiology, including the regulation of vascular tone, neurotransmission, and immune responses.[37,38] In the eye, NO facilitates the relaxation of the TM and Schlemm's canal, enhancing the outflow of aqueous humor through the conventional pathway. This reduction in outflow resistance effectively lowers IOP. Latanoprostene bunod, a glaucomatous eye drop, leverages this property by releasing NO, which directly relaxes the TM, thereby improving aqueous humor drainage and reducing IOP through a NO-mediated mechanism.[39,40]

Direct interactions between ECM synthesis and NO transport in the TM have not been extensively characterized. However, several potential mechanisms may link these processes. First, the composition and organization of ECM within the TM influence its permeability and hydraulic conductivity. Changes in ECM synthesis can alter TM architecture, potentially affecting aqueous humor outflow dynamics. NO can modulate vascular tone and smooth muscle relaxation within the TM, thereby influencing tissue permeability and aqueous humor flow. Second, both ECM components and NO signaling pathways can influence cellular behavior within the TM. ECM proteins, such as collagen, fibronectin, and laminin, provide structural support and signaling cues for TM cells, affecting cell adhesion, migration, and differentiation. NO signaling, on the other hand, regulates cellular processes such as cytoskeletal dynamics, gene expression, and cell-cell communication. Therefore, cross-talk between ECM and NO signaling may modulate cellular responses within the TM.[38]

5. CONCLUSION

In this study, we investigated the potential of BMP-7 as a therapeutic agent to inhibit ECM buildup, a key factor in the development of steroid-induced glaucoma. Our results demonstrated that BMP-7 effectively suppresses ECM accumulation, indicating its potential for both the prevention and treatment of this condition. Additionally, we identified specific genes involved in the ECM reduction process, contributing to a deeper understanding of the molecular mechanisms underlying steroid-induced glaucoma. This research suggests that BMP-7 could serve as a valuable clinical therapy for managing the progression of this disease.

This study was conducted in vitro, and the potential in vivo toxicity of BMP-7 remains to be tested. Further research is necessary to determine the appropriate dose and assess any potential side effects of BMP-7 in humans.

REFERENCES

1. Liesenborghs I, Eijssen LMT, Kutmon M, et al. The Molecular Processes in the Trabecular Meshwork After Exposure to Corticosteroids and in Corticosteroid-Induced Ocular Hypertension. *Invest Ophthalmol Vis Sci.* 2020;61(4):24.
2. Cho WJ, Lee JM, Bae HW, Kim CY, Seong GJ, Choi W. Baseline intraocular pressure: an independent risk factor in severe steroid-induced ocular hypertension after intravitreal dexamethasone implant. *Graefes Arch Clin Exp Ophthalmol.* 2024;262(4):1231-1243.
3. Choi W, Kim JD, Bae HW, Kim CY, Seong GJ, Kim M. Axial Length as a Risk Factor for Steroid-Induced Ocular Hypertension. *Yonsei Med J.* 2022;63(9):850-855.
4. Phulke S, Kaushik S, Kaur S, Pandav S. Steroid-induced glaucoma: an avoidable irreversible blindness. *Journal of current glaucoma practice.* 2017;11(2):67.
5. Cho WJ, Kim Y, Kim JD, et al. Association of trabecular meshwork height with steroid-induced ocular hypertension. *Sci Rep.* 2023;13(1):9143.
6. Vranka JA, Kelley MJ, Acott TS, Keller KE. Extracellular matrix in the trabecular meshwork: intraocular pressure regulation and dysregulation in glaucoma. *Exp Eye Res.* 2015;133:112-125.
7. Acott TS, Kelley MJ. Extracellular matrix in the trabecular meshwork. *Exp Eye Res.* 2008;86(4):543-561.
8. Fleenor DL, Shepard AR, Hellberg PE, Jacobson N, Pang IH, Clark AF. TGFbeta2-induced changes in human trabecular meshwork: implications for intraocular pressure. *Invest Ophthalmol Vis Sci.* 2006;47(1):226-234.
9. Fuchshofer R, Tamm ER. The role of TGF-beta in the pathogenesis of primary open-angle glaucoma. *Cell Tissue Res.* 2012;347(1):279-290.
10. Pervan CL. Smad-independent TGF-beta2 signaling pathways in human trabecular meshwork cells. *Exp Eye Res.* 2017;158:137-145.
11. Fuchshofer R, Yu AH, Welge-Lussen U, Tamm ER. Bone morphogenetic protein-7 is an antagonist of transforming growth factor-beta2 in human trabecular meshwork cells. *Invest Ophthalmol Vis Sci.* 2007;48(2):715-726.
12. Kim S, Shin DH, Nam BY, et al. Newly designed Protein Transduction Domain (PTD)-mediated BMP-7 is a potential therapeutic for peritoneal fibrosis. *Journal of Cellular and Molecular Medicine.* 2020;24(22):13507-13522.
13. Lee K-M, Suh JW, Ko E, et al. Lipid Nanoparticle Formulated Protein Transduction Domain-Bone Morphogenetic Protein-2 Enhances Wound Healing in Type 1 Diabetic Mice. *Available at SSRN 4284407.*
14. Kim S, Jeong CH, Song SH, et al. Micellized Protein Transduction Domain-Bone Morphogenetic Protein-7 Efficiently Blocks Renal Fibrosis Via Inhibition of Transforming Growth Factor-Beta-Mediated Epithelial-Mesenchymal Transition. *Front Pharmacol.* 2020;11:591275.
15. Jeong CH, Lim S-Y, Um JE, et al. Micellized protein transduction domain-bone morphogenetic protein-2 accelerates bone healing in a rat tibial distraction osteogenesis model. *Acta Biomaterialia.* 2023;170:360-375.
16. Kim NH, Cha YH, Kim HS, et al. A platform technique for growth factor delivery with novel mode of action. *Biomaterials.* 2014;35(37):9888-9896.

17. Choi W, Lee MW, Kang HG, et al. Comparison of the trabecular meshwork length between open and closed angle with evaluation of the scleral spur location. *Sci Rep.* 2019;9(1):6857.
18. Choi W, Bae HW, Cho H, Kim EW, Kim CY, Seong GJ. Evaluation of the Relationship Between Age and Trabecular Meshwork Height to Predict the Risk of Glaucoma. *Sci Rep.* 2020;10(1):7115.
19. Clark AF, Brotchie D, Read AT, et al. Dexamethasone alters F-actin architecture and promotes cross-linked actin network formation in human trabecular meshwork tissue. *Cell motility and the cytoskeleton.* 2005;60(2):83-95.
20. Steely HT, Browder SL, Julian MB, Miggans ST, Wilson KL, Clark AF. The effects of dexamethasone on fibronectin expression in cultured human trabecular meshwork cells. *Investigative ophthalmology & visual science.* 1992;33(7):2242-2250.
21. Group CATTS, Khaw P, Grehn F, et al. A phase III study of subconjunctival human anti-transforming growth factor beta(2) monoclonal antibody (CAT-152) to prevent scarring after first-time trabeculectomy. *Ophthalmology.* 2007;114(10):1822-1830.
22. Mead AL, Wong TT, Cordeiro MF, Anderson IK, Khaw PT. Evaluation of anti-TGF-beta2 antibody as a new postoperative anti-scarring agent in glaucoma surgery. *Invest Ophthalmol Vis Sci.* 2003;44(8):3394-3401.
23. Tovar-Vidales T, Clark AF, Wordinger RJ. Transforming growth factor-beta2 utilizes the canonical Smad-signaling pathway to regulate tissue transglutaminase expression in human trabecular meshwork cells. *Exp Eye Res.* 2011;93(4):442-451.
24. Meng X-M, Chung AC, Lan HY. Role of the TGF-β/BMP-7/Smad pathways in renal diseases. *Clinical science.* 2013;124(4):243-254.
25. Koh ES, Chung S. Recent Update on Acute Kidney Injury-to-Chronic Kidney Disease Transition. *Yonsei Med J.* 2024;65(5):247-256.
26. Liu P, Zhu L, Zou G, Ke H. Matrine Suppresses Pancreatic Fibrosis by Regulating TGF-beta/Smad Signaling in Rats. *Yonsei Med J.* 2019;60(1):79-87.
27. Yao H, Ge T, Zhang Y, et al. BMP7 antagonizes proliferative vitreoretinopathy through retinal pigment epithelial fibrosis in vivo and in vitro. *FASEB J.* 2019;33(3):3212-3224.
28. Messenger SW, Falkowski MA, Thomas DD, et al. Vesicle associated membrane protein 8 (VAMP8)-mediated zymogen granule exocytosis is dependent on endosomal trafficking via the constitutive-like secretory pathway. *Journal of Biological Chemistry.* 2014;289(40):28040-28053.
29. Soles A, Selimovic A, Sbrocco K, et al. Extracellular matrix regulation in physiology and in brain disease. *International journal of molecular sciences.* 2023;24(8):7049.
30. Ji L, Xu S, Luo H, Zeng F. Insights from DOCK2 in cell function and pathophysiology. *Frontiers in molecular biosciences.* 2022;9:997659.
31. Zatulovskiy E, Zhang S, Berenson DF, Topacio BR, Skotheim JM. Cell growth dilutes the cell cycle inhibitor Rb to trigger cell division. *Science.* 2020;369(6502):466-471.
32. Seabra MC, Mules EH, Hume AN. Rab GTPases, intracellular traffic and disease. *Trends in molecular medicine.* 2002;8(1):23-30.
33. Chong CE, Lim KP, Gan CP, et al. Over-expression of MAGED4B increases cell migration and growth in oral squamous cell carcinoma and is associated with poor disease outcome. *Cancer letters.* 2012;321(1):18-26.
34. Liu C, Liu J, Shao J, et al. MAGED4B Promotes Glioma Progression via Inactivation of the TNF-α-induced Apoptotic Pathway by Down-regulating TRIM27 Expression. *Neuroscience Bulletin.* 2023;39(2):273-291.

35. Zhao X, Ramsey KE, Stephan DA, Russell P. Gene and protein expression changes in human trabecular meshwork cells treated with transforming growth factor-beta. *Invest Ophthalmol Vis Sci.* 2004;45(11):4023-4034.
36. Youngblood H, Cai J, Drewry MD, et al. Expression of mRNAs, miRNAs, and lncRNAs in Human Trabecular Meshwork Cells Upon Mechanical Stretch. *Invest Ophthalmol Vis Sci.* 2020;61(5):2.
37. Ignarro LJ, Cirino G, Casini A, Napoli C. Nitric oxide as a signaling molecule in the vascular system: an overview. *Journal of cardiovascular pharmacology.* 1999;34(6):879-886.
38. Rosselli M, Keller R, Dubey RK. Role of nitric oxide in the biology, physiology and pathophysiology of reproduction. *Human reproduction update.* 1998;4(1):3-24.
39. Cavet ME, Vittitow JL, Impagnatiello F, Ongini E, Bastia E. Nitric oxide (NO): an emerging target for the treatment of glaucoma. *Investigative ophthalmology & visual science.* 2014;55(8):5005-5015.
40. Garhöfer G, Schmetterer L. Nitric oxide: a drug target for glaucoma revisited. *Drug Discovery Today.* 2019;24(8):1614-1620.

Abstract in Korean

스테로이드에 의해 유도된 인간 섬유주 세포에서의 세포외기질 합성에 대한 뼈형성단백질-7의 효과

목적 : 이 연구는 스테로이드에 의해 유도된 인간 섬유주 세포에서의 세포외 기질 합성에 대한 뼈형성단백질-7 의 효과를 조사하고자 하였습니다. 스테로이드는 안과 질환 치료에 필수적이지만, 장기 사용 시 안압 증가 및 녹내장 위험을 초래할 수 있습니다. 스테로이드 유발 녹내장은 세포외 기질 축적에 의한 안압상승에 기인 하는 것으로 알려져 있습니다. 따라서 본 연구는 스테로이드로 유발된 섬유주 내 세포외 기질 축적을 억제하는 보호 물질로서 뼈형성단백질-7 의 가능성을 탐구하고자 하였습니다

방법 : 인간 섬유주 세포에서 스테로이드 단독 처리 또는 스테로이드와 뼈형성단백질-7 병용 처리로 나누어 세포외 기질 생성에 미치는 영향을 비교하였습니다. 뼈형성단백질-7 은 변형 성장 인자 베타의 길항제로 알려져 있으며, 생물학적 활성을 강화하기 위해 미셀화된 단백질 전달 도메인이 결합된 뼈형성단백질-7 폴리펩타이드 형태로 처리 되었습니다. 또한, 유전자 발현 분석을 통해 세포외 기질 조절에 관여하는 특정 유전자들을 확인하였습니다.

결과 : 연구 결과, 뼈형성단백질-7 은 스테로이드에 의해 유도된 세포외 기질 축적을 효과적으로 억제하였습니다. 스테로이드와 뼈형성단백질-7 병용 처리군은 스테로이

드 단독 처리군에 비해 세포외 기질 생성이 유의미하게 감소하였습니다. 추가로, 뼈형성단백질-7의 세포외 기질 조절 과정에 관여하는 여러 핵심 유전자들이 염기서열분석을 통해 확인되었습니다.

결론 : 본 연구는 뼈형성단백질-7 이 스테로이드로부터 유도된 세포외 기질 합성을 억제하여 인간 섬유주 세포에서 보호적이며 항섬유화 효과를 발휘한다는 증거를 제시합니다. 이러한 연구 결과는 뼈형성단백질-7 이 스테로이드 유발 녹내장을 예방하거나 치료하는 데 있어 유망한 치료 표적으로 작용할 수 있음을 시사하며, 정상적인 안구방수 흐름을 유지하고 안압 상승을 방지하는 데 도움이 될 것으로 기대됩니다.

핵심되는 말 : 스테로이드, 녹내장, 섬유주, 세포외기질, 뼈형성단백질-7

\